EXTENDED PDF FORMAT
SPONSORED BY

BIO-RAD

http://discover.bio-rad.com

Applications of Modern Ferroelectrics

J. F. Scott, *et al.*

Science **315**, 954 (2007);
DOI: 10.1126/science.1129564

The following resources related to this article are available online at www.sciencemag.org (this information is current as of March 1, 2007):

Updated information and services, including high-resolution figures, can be found in the online version of this article at:
http://www.sciencemag.org/cgi/content/full/315/5814/954

This article **cites 14 articles**, 4 of which can be accessed for free:
http://www.sciencemag.org/cgi/content/full/315/5814/954#otherarticles

This article appears in the following **subject collections**:
Materials Science
http://www.sciencemag.org/cgi/collection/mat_sci

Information about obtaining **reprints** of this article or about obtaining **permission to reproduce this article** in whole or in part can be found at:
http://www.sciencemag.org/about/permissions.dtl

Downloaded from www.sciencemag.org on March 1, 2007

Science (print ISSN 0036-8075; online ISSN 1095-9203) is published weekly, except the last week in December, by the American Association for the Advancement of Science, 1200 New York Avenue NW, Washington, DC 20005. Copyright c 2007 by the American Association for the Advancement of Science; all rights reserved. The title SCIENCE is a registered trademark of AAAS.

Applications of Modern Ferroelectrics

J. F. Scott

Long viewed as a topic in classical physics, ferroelectricity can be described by a quantum mechanical ab initio theory. Thin-film nanoscale device structures integrated onto Si chips have made inroads into the semiconductor industry. Recent prototype applications include ultrafast switching, cheap room-temperature magnetic-field detectors, piezoelectric nanotubes for microfluidic systems, electrocaloric coolers for computers, phased-array radar, and three-dimensional trenched capacitors for dynamic random access memories. Terabit-per-square-inch ferroelectric arrays of lead zirconate titanate have been reported on Pt nanowire interconnects and nanorings with 5-nanometer diameters. Finally, electron emission from ferroelectrics yields cheap, high-power microwave devices and miniature x-ray and neutron sources.

From their discovery by Valasek in 1920 until about 1943, ferroelectrics were academic curiosities, of little application or theoretical interest, mostly water-soluble and fragile. They were all hydrogen bonded and were thought to be essential for ferroelectricity. During the war years, this changed upon the discovery of the robust ferroelectric oxide $BaTiO_3$ (*1*), whose structural simplicity encouraged theoretical work and whose physical properties stimulated engineering devices; thus, ferroelectric oxides became an "electronic ceramics" industry. Billions of $BaTiO_3$ "condensers" are still made annually, at a cost of less than one cent per capacitor, even including expensive Ag/Pd electrodes.

Before 1970, the most exciting challenge in ferroelectrics was modeling ferroelectric phase transitions (*2*) and discovering new ones. There are now 700 ferroelectric materials, many of which are neither hydrogen bonded nor oxides, such as GeTe, $SrAlF_5$, or SbSI (*3*, *4*). Because of the high cost of single crystals, devices were limited to bulk ceramics. These were very successful for actuators and piezoelectric transducers as well as for pyroelectric detectors. The application to sonar was especially well funded.

The focus changed after 1984, when thin-film ferroelectrics were developed and first integrated into semiconductor chips (*5*). In 1994, a ferroelectric bypass capacitor for 2.3-GHz operation in mobile digital telephones won the Japan Electronic Industry "Product of the Year" award, with 6 million chips per month in production. The polarization of a typical ferroelectric is reversed at a critical "coercive" field $E \approx 50$ kV/cm. In a 1-mm bulk device, this is a 5-kV voltage unsuitable for a mobile telephone; however, for submicrometer films it is <5 V, permitting integration into most silicon chips. It is in the form of "integrated ferroelectrics" that the renaissance of ferromaterials occurred. The first Review in *Science* of integrated ferroelectrics (*5*) was published in 1989, and the first text on ferroelectric memories (*6*) was published in 2000 and then translated into Japanese (2003) and Chinese (2004), reflecting the locations of greatest current activity. Ferroelectricity is now treated by a quantum mechanical Berry-phase formalism; such an ab initio approach is compatible with magnetic calculations in the same materials, stimulating a renaissance in magnetoelectric materials that are simultaneously ferromagnetic and ferroelectric (*7*, *8*).

There are several directions for ferroelectrics research: substrate-film interfaces and high-strain states, finite size effects, nanotubes and nanowires, electrocaloric devices, ferroelectric random access memories (FeRAMs), dynamic random access memory (DRAM) capacitors, electron emitters, weak–magnetic field sensors, magnetoelectrics, and self-assembly. Ferroelectric liquid crystals (smectic thin films) probably have a more mature commercial product line (spatial light modulators and video camera view-finders) but are not included in this Review.

A ferroelectric is generally defined as a material whose intrinsic lattice polarization P can be reversed through the application of an external electric field E that is greater than the coercive field E_c. Ferroelectrics usually have a phase-transition temperature T_0 above which they are paraelectric, but some do not (they melt first). All ferroelectrics are also pyroelectric, and all pyroelectrics are piezoelectric. (The reverse is not true: Pyroelectric ZnO is not ferroelectric.) Hence, ferroelectrics cannot have a center of symmetry nor can they be glasses. In their paraelectric phase, some are centrosymmetric ($BaTiO_3$) and some are not (KH_2PO_4). Most ferroelectric families are not oxides, though these are most studied because of their robustness and practical applications. Not all solids with electrical hysteresis are ferroelectric: Electrets have an extrinsic hysteresis due to mobile charged defects, and pn-junctions also exhibit hysteresis. Measuring polarization P is often contaminated with artifacts: For perfectly insulating capacitors, apply E and measure switched charge $Q = 2PA$, where P is polarization and A is electrode area. However, in semiconducting or lossy dielectrics $Q = \sigma AVt/d + 2PA$, where σ is conductivity, t is time, and V is voltage across thickness d. Real charge is injected. Losses result in a cigar-shaped loop that is unrelated to ferroelectricity. Although one looks for flat, saturated hysteresis curves, these can be artifacts also, resulting from saturated amplifiers. dP/dV in a hysteresis curve cannot be perfectly flat; that would imply an unphysical dielectric constant of zero.

Ferroelectric Nanostructures

There are two research and development (R&D) thrusts in nanoferroelectrics. First, are there physical phenomena such as crystallographic phases or domain structures that are stable only at these sizes? Second, are the nanoscale device properties qualitatively different? One might examine ferroelectric quantum dots and confinement energies, direct electron tunneling, unusual phases resulting from substrate-interface strain, and transport properties of semiconducting ferroelectrics. Typical oxide ferroelectrics are wide-gap semiconductors with band gaps $E_g = 3.5$ to 4.1 eV and both electronic and ionic conduction. Most are p-type as grown. Electron mobilities are low (0.1 to 3.0 $cm^2/V\cdot s$); ionic mobilities (e.g., oxygen vacancies) are about 10^{-12} $cm^2/V\cdot s$; and effective masses are high ($m^* = 5.0$ to 6.7 m_e). Lead zirconate-titanate (PZT), strontium bismuth tantalate (SBT), and bismuth titanate (BiT) are switching-device favorites (*9*), and barium strontium titanate (BST) is used for nonswitching applications.

Exactly 60 years ago, Kittel published a paper (*10*) showing that 180° magnetic domains exhibit stripe widths w that are proportional to the square root of the crystal thickness d: $w^2 = a'd$, where a' expresses a balance between domain wall energy and surface energy. More recently, Catalan *et al.* (*11*) and Lukyanchuk *et al.* (*12*) have shown that $w^2 = ad\mathrm{T}$, where T is the domain wall thickness and $a = \{2\pi^3/[21\zeta(3)]\}\ [\chi(z)/\chi(x)]^{1/2} = 2.455\ [\chi(z)/\chi(x)]^{1/2}$, where $\chi(x,y,z)$ are the susceptibilities and $\zeta(3)$ is the Riemann zeta function of power 3. This dimensionless equation is universal, applying equally to magnets and ferroelectrics (Fig. 1A).

The Kay-Dunn Law similarly describes the coercive field $E_c = bd^{-2/3}$ and coercive voltage $V_c = bd^{1/3}$. Both of these laws hold from macroscopic millimeter thickness d down to about 2 nm. Thus, surprisingly, much of the behavior of nanoferroelectric domains can be derived from bulk classical physics. Domains are usually studied in flat planes, but some three-dimensional (3D) nanodomains are shown in Fig. 1B. Domain switching in submicrometer ferroelectrics is rate-limited by nucleation rather than by domain wall velocities, unlike bulk, and can be <280 ps.

Figure 1, C and D, shows nanostructures in thin ceramic films: Figure 1C shows nanotubes and Fig. 1D shows a 0.3 terabit/inch^2 (Tb/in^2) nanoarray of Pt nanowires per PZT (1 Tb/in^2 = 1600 Tb/m^2). In Fig. 2, more complex nanodevice structures are shown: Figure 2A is a magnetoelectric composite electron micrograph

Centre for Ferroics, Earth Sciences Department, University of Cambridge, Cambridge CB2 3EQ, UK. E-mail: jsco99@esc.cam.ac.uk

Downloaded from www.sciencemag.org on March 1, 2007

(*13*), and Fig. 2B shows nanowriting of patterns with an atomic force microscopy (AFM) tip (*14*).

Terabit ferroelectric memories are not quite a reality; the state-of-the-art hard-wired device is a 0.3 Tb/in^2 PZT array (*15*) on Pt nanowires encased in mesoporous Al_2O_3. These unregistered 30-nm-diameter capacitors switch a readable 2000 electrons per bit, and fully registered alumina pores are available. Figure 2 shows nanoferroelectrics fabricated as composites (Fig. 2A), from AFM writing (Fig. 2B), and through a focused ion beam (FIB) (Fig. 2, C and D). Scientists in Belfast have fabricated complicated 3D nanostructures, including (*16*) FIB-cut free-standing microrings (Fig. 2C), and a 5-nm inside-diameter PZT nanoring (Fig. 2D), solution-deposited within a pore of mesoporous Si (*17*). Using synchrotron sources (Fig. 3A), one can study the domain structure of such very thin films. The 2004 32–megabit (Mb) FeRAMs from Samsung (PZT) or Matsushita (SBT) are still ahead of the commercial magnetic random access memory (MRAM) development (4-Mb MRAM from Freescale CO, July 2006), and Samsung now has a 64-Mb FeRAM. A more advanced ferroelectric-gate field-effect transistor (FET) offers nondestructive read operation, but short retention times have thus far precluded commercial products.

Symetrix and Matsushita Electronics Corporation (MEC) have produced SBT FeRAMs with breakdown of 1.5 MV/cm for the semiconductor 45-nm node (DRAM half-pitch; 2010 target). FeRAMs are produced at 25,000 on each 8-inch Si wafer, with 6 million per month shipped for applications such as Japanese Railroad "smart" fare cards. Ramtron and Fujitsu are at 0.35-μm strap-cell PZT design; MEC has produced 500 million units of SBT thin-film integrated ferroelectrics (1 billion, including nonswitching BST-on-GaAs capacitors) and is at 0.13-μm stacked 4-level-metal design. The Symetrix 5-ns access-time "Trinion" cell is the first nonvolatile cache memory. On 15 December 2006, Fujitsu announced production of a Mn-doped $BiFeO_3$ memory for the 65-nm node.

Self-Patterning

The two basic ways of fabricating nanoferroelectric devices are "top down" (submicrometer lithography) and "bottom up" (self-assembly). The development of mesoporous Si, Al_2O_3, GaN, and GaAs has presented experimentalists with templates for the latter, and other techniques for coating nanowires have developed. Self-assembly of nanoelectrodes on ferroelectric films (*18*) (Fig. 3B) is based on the model of Andreev that such islands would repel each other through their mutual strain interactions with the substrate. Complete registration that is satisfactory for commercial RAM memory devices can be achieved through deposition with inert spacers, such as submicrometer silicon spheres.

True finite-size depolarization effects were once thought, incorrectly, to occur at dimensions slightly less than 100 nm. In nanospheres of $BaTiO_3$, the outside shell is cubic (paraelectric) and the interior is (*19*) tetragonal and ferroelectric (thus resembling an M&M candy). As diameter is reduced, the nanosphere is all cubic and not ferroelectric, but this is just a surface chemistry effect and not a finite size effect. Real finite size effects may occur for diameters that are <3 nm.

Most readers are familiar with carbon nanotubes. These are generally good conductors, either metallic or semiconducting. By comparison, ferroelectric nanotubes are fairly good insulators. When a voltage is applied to them, they expand, contract, or bend (piezoelectric). First fabricated by Hernandez in Colorado and Mishina in Moscow, such oxide nanotubes have recently been characterized by Morrison *et al.* (*20*). Notably, the size distribution of self-assembled nano-islands of PZT in Fig. 3B is not a phase diagram (it is not a system in thermal equilibrium). Figure 3, C to E, shows true phase diagrams for nanoferroelectrics.

The distribution function for fractional percentage w of islands of a certain volume V has

$$\log(w) = a_0V + b_0V^{1/3} + c_0V^{2/3} \quad (1)$$

assumed, with empirical parameters a_0, b_0, and c_0.

Magnetoelectrics

Crystals whose Hamiltonians contained linear coupling between electric polarization P and

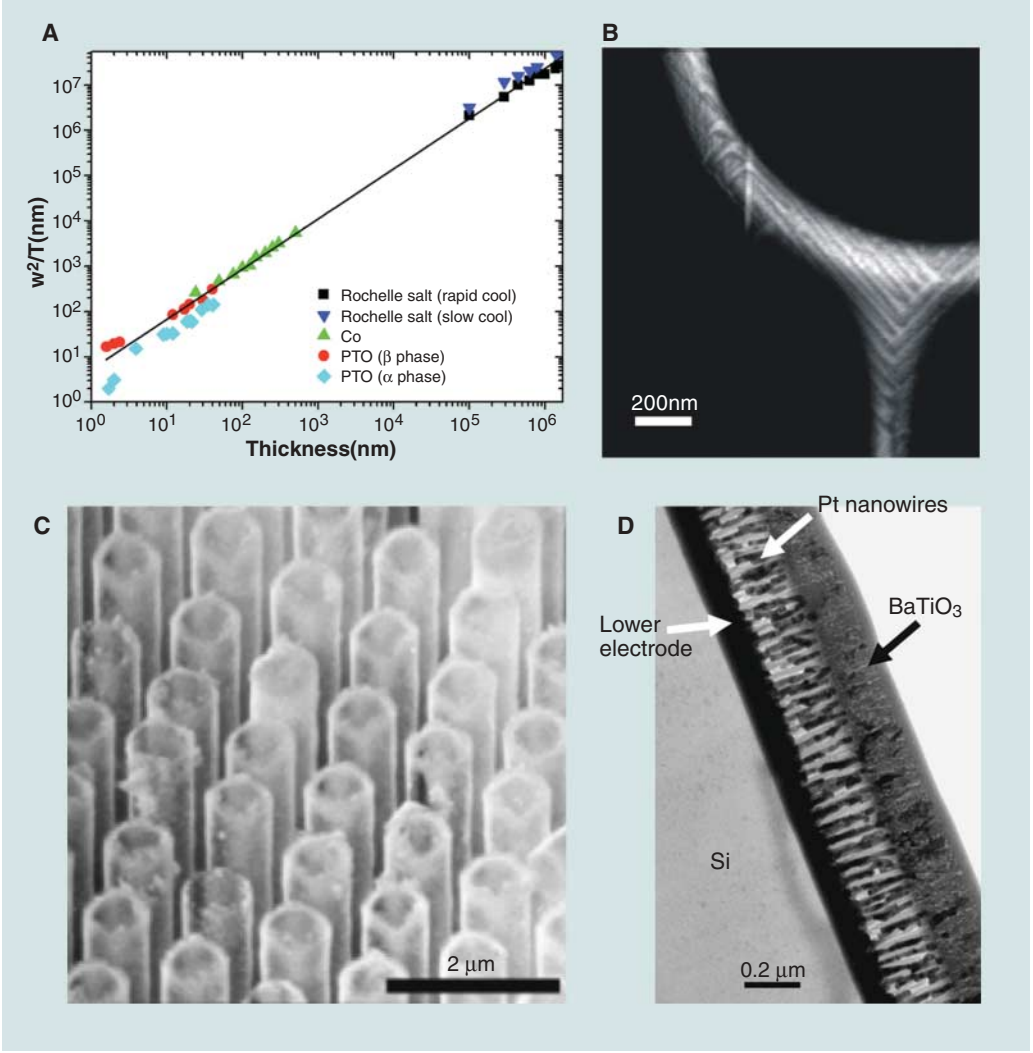

Fig. 1. Nanostructures in thin ceramic films. (**A**) Stripe width squared divided by domain wall thickness T versus film thickness d, showing that w^2/dT is constant in ferroelectrics $PbTiO_3$ and $BaTiO_3$ and in Rochelle Salt and ferromagnet Co, demonstrating a universal law over 6 decades (*49*). (**B**) Plan view micrograph of 3D nanodomains in $BaTiO_3$ (*16*). (**C**) Scanning electron microscopy (SEM) micrograph of $SrBi_2Ta_2O_9$ nanotubes at oblique incidence (*20*). (**D**) SEM cross-sectional view of 0.5 Tb/in^2 nanoarray of Pt nanowires and PZT (*15*).

Downloaded from www.sciencemag.org on March 1, 2007

magnetization M were thought to be discovered in France in the 1920s. However, after subsequent data showed that the effect was forbidden in the materials used, it was believed impossible, causing a hiatus in "magnetoelectricity" R&D until 1957, when Moscow groups resurrected the problem. Dzyaloshinskii predicted magnetoelectricity in Cr_2O_3, rapidly confirmed by Astrov, and also piezomagnetism, quickly found by Borovik-Romanov. During the 1970s, a successful search for linear magnetoelectrics ("multiferroics") was led by Hans Schmid in Geneva. The primary device interest was multistate logic elements for computer bit storage that could be greater than binary. As such, it was imperative to show switching of magnetic states with electric fields and/or of ferroelectric states with magnetic fields and the interaction between magnetic and electric domain walls. This work has had a renaissance since 2000, emphasizing manganese and terbium compounds (*7*, *8*).

Magnetoelectricity studies emphasize two terms, which are given in Eq. 2:

$$H = \alpha_{ij} \langle P_i \rangle \langle M_j \rangle + \beta_{ijk} \langle P_i \rangle \langle M_j M_k \rangle \quad (2)$$

where P is electric polarization and M is magnetization. The first term is not time-reversal invariant. Here, the linear magnetoelectric effect due to α_{ij} vanishes above T_N (the Neel temperature) or T_c (the Curie temperature), because $\langle M \rangle = 0$; however, the quadratic term due to β_{ijk} is proportional to $\langle M^2 \rangle$ and remains finite well above T_N (until $T \approx 3T_N$ in magnets such as $BaMnF_4$ with 2D planar spin ordering).

To switch a magnetic domain with an electric field, we need to know how much the magnetization M depends on the polarization P. Does reversing P influence M by 1, 10, or 100%? The idea that ferroelectricity could actually cause ferromagnetism (a 100% effect) was explained by Fox and Scott in 1977 (*21*) and exemplified with the $BaMF_4$ family (M = Mn, Ni, Co, and Fe). By producing a weak ferromagnetic moment (canting of antiferromagnetic spin sublattices) $M_i = \alpha_{ij} P_j$ through the Dzyaloshinskii-Moriya anisotropic exchange, the ferroelectric polarization can produce this effect in some point symmetry groups (e.g., 2′ in $BaMnF_4$) but not others (e.g., 2 in $BaCoF_4$). The angle of spin canting (3 mrad = 0.17° in $BaMnF_4$) implies a plausible value for the anisotropic exchange in comparison with off-diagonal α_{ij} in other Mn^{+2} compounds). This Fox-Scott model has recently been discussed for $BaNiF_4$ (*22*).

There are artifact problems in the recent magnetoelectric literature. Strong magnetocapacitance (dielectric constant change with applied magnetic field) can occur merely through Maxwell-Wagner space charge in any magnetoresistive material (*11*). This is not intrinsic and requires no ferroelectricity at all. The effects can be huge and may explain the 450% anomaly in cadmium (or mercury) chromium spinel (*23*).

Brown, Hornreich, and Shtrikman showed that the square of the magnetoelectric susceptibility cannot exceed the product of the electric susceptibility and the magnetic susceptibility, $\chi_{me}^2 \leq \chi_m \chi_e$, making it uselessly weak for devices. However, that ignores indirect coupling through strain. Strain coupling can be within a single material, or it can involve two materials in intimate proximity. By choosing two materials in a laminated or nanostructured bimorph, one can cause large magnetostriction in, for example, terphenyl-d, and large piezoelectricity in, for example, PZT. The result is a prototype room-temperature detector of weak magnetic fields—a low-cost (uncooled) replacement for superconducting quantum interference device (SQUID) detectors. Unfortunately, the "Holy Grail" of multiferroics—a strong (uncanted) ferromagnet that is also ferroelectric at room temperature—has yet to be found. As a memory element, it would permit electric write operation and magnetic read, eliminating the need for a destructive read (and reset) for present-day FeRAMs and making possible fatigue-free memories. This attractive possibility requires a ferroelectric that is also a strong ferromagnet and has low electrical conductivity at ambient temperatures. Although $BiFeO_3$ doped to increase resistivity remains a possible candidate, ferroelectric-ferromagnetic fluorides such as $A_3(MF_6)_2$ or $K_3Fe_5F_{15}$ merit much more study (*5*), where A is Sr or Pb and M is any 3d metal (Ti, V, Cr, or Fe); these are apparently ferroelectric with dielectric peaks at $550\ K < T_c < 740\ K$.

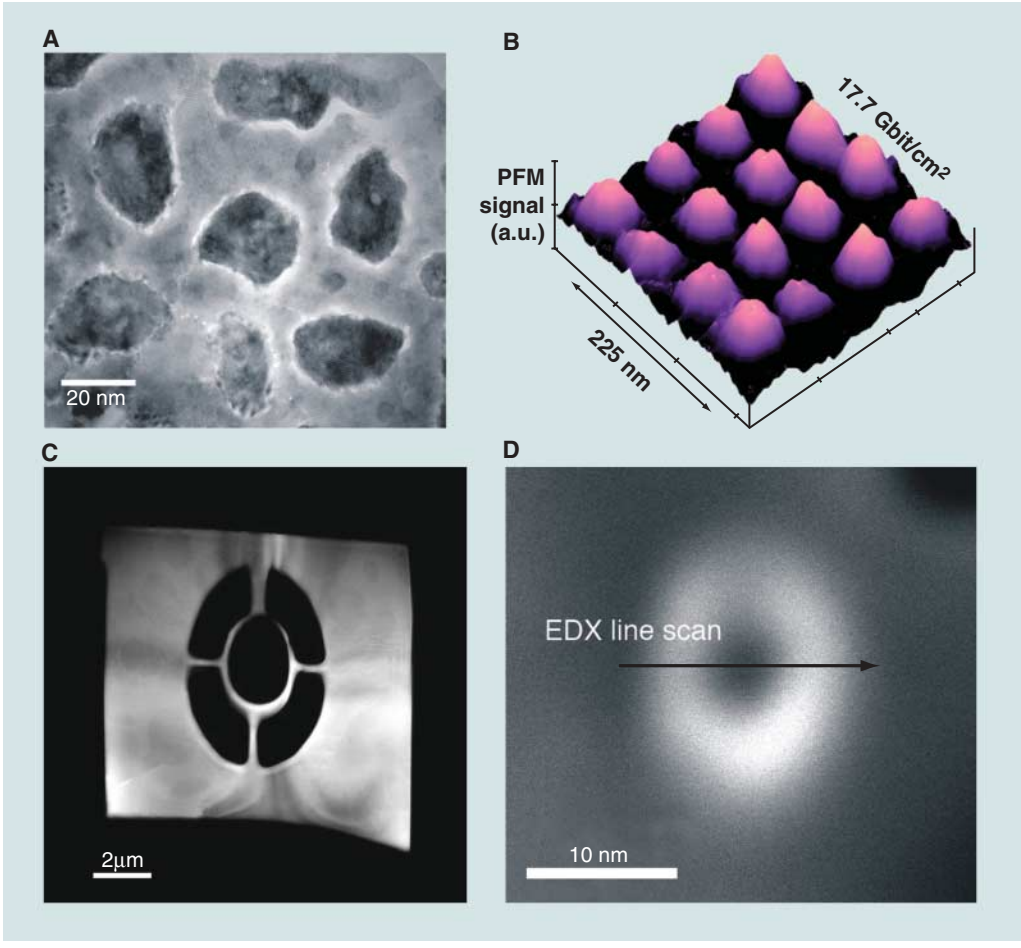

Fig. 2. FIB nanoscience. (**A**) SEM plan view of magnetoelectric composite of $CoFe_2O_4$ pillars in a $BaTiO_3$ matrix (*13*). (**B**) Nanodomains produced by AFM nanowriting on PZT (*50*). a.u., arbitrary units. (**C**) Electron micrograph of nanotoroid of single-crystal $BaTiO_3$ (*15*). (**D**) Micrograph of ultra-nanotoroid of PZT inside a mesoporous Al_2O_3 pore (*17*). EDX, energy-dispersive x-ray analysis.

Toroidal and Circular Ordering of Ferroelectric Domains

Most ferroelectrics or antiferroelectrics order with polarizations that are parallel or antiparallel, respectively. However, circular or toroidal patterns can occur. As Kittel first pointed out (*10*), ferromagnets in nanosize diameters will order with four 90° do-

Downloaded from www.sciencemag.org on March 1, 2007

mains, forming a circle. This kind of topological spin defect (vortex) was treated theoretically by Mermin (*24*) in terms of winding numbers and is commonly found in nanomagnets, including both naturally occurring minerals and synthetics (*25*).

A completely different origin for circular or toroidal domains occurs in magnetoelectrics, even in bulk. First analyzed in detail by Ginzburg and by Sannikov, this is reviewed by several authors (*7*, *8*) and subject to a flurry of recent papers, but not yet unambiguously observed. Such a system offers the possibility of very high-density (Tb/in^2) memory and storage with electrical write (fast) and magnetic read (no reset).

Ab Initio Theory

A veritable renaissance in theoretical ferroelectricity has resulted from the work by Resta, Vanderbilt, Rabe, Cohen, Krakauer, and others on ab initio models. These replace the semiclassical ball-and-stick model with fully quantum mechanical calculations. They have proved particularly insightful in calculating temperature-strain phase diagrams for thin films (*26*), in which the large strains result from coherent (epitaxial) growth onto substrates with slightly different lattice constants from those of the ferroelectric film (Fig. 3, C to E). The technique suffers from four limitations: (i) It generally works for zero applied field *E*, although Wu *et al.* have done finite field calculations (*27*). (ii) Most work is at zero temperature. (iii) The number of atoms in the programs are still too small even for nanodevice simulations. (iv) It is not easy to incorporate the semiconducting character of the ferroelectric oxides, nor defects such as oxygen vacancies, nor gradients near the electrode interface.

One of the most important qualitative things to come from these new models is the prediction shown in Fig. 3 from Pertsev and Tagantsev *et al.* (*28*) that a new *ac* phase occurs with polarization lying between the *a* and *c* faces of a pseudo-tetragonal $BaTiO_3$ crystal. If correct, this would have been new physics. Unfortunately, the ab initio work of Vanderbilt (Fig. 3E) shows that both models of Pertsev and Tagantsev *et al.* (Fig. 3, C and D) are qualitatively wrong and that there is no *ac* phase (*27*). This shows the power of ab initio modeling over more primitive free-energy theories. Although the Pertsev-Tagantsev model was unsuccessful for barium titanate, a more successful example is $PbTiO_3$, which in bulk has only cubic and tetragonal phases but in thin film exhibits both an orthorhombic phase (*aa*, meaning that polarization *P* lies at a 45° angle from each of the two *a* axes of the tetragonal precursor phase, along [110]) and a rhombohedral (r) phase (*P* along [111]). For $BaTiO_3$ the initial model predictions were that a new *ac* phase would be stable in thin-film form at zero stress, but ab initio calculations (*29*) showed that this is unlikely. The most extreme experimental result is that $SrTiO_3$, which in bulk is paraelectric down to absolute zero, can be made ferroelectric at room temperature in thin-film form (*30*) with the use of a rather new substrate material: $DyScO_3$.

Interfacial phenomena. Ferroelectrics are more complicated than ferromagnets because electrical measurements must be made on a sandwich consisting of two electrodes around a dielectric. The interface is very complex, involving screening in the metal (*31*) and instabilities at about 3 nm of dielectric thickness (*32*). The resulting leakage current in PZT films can be Schottky-limited or Poole-

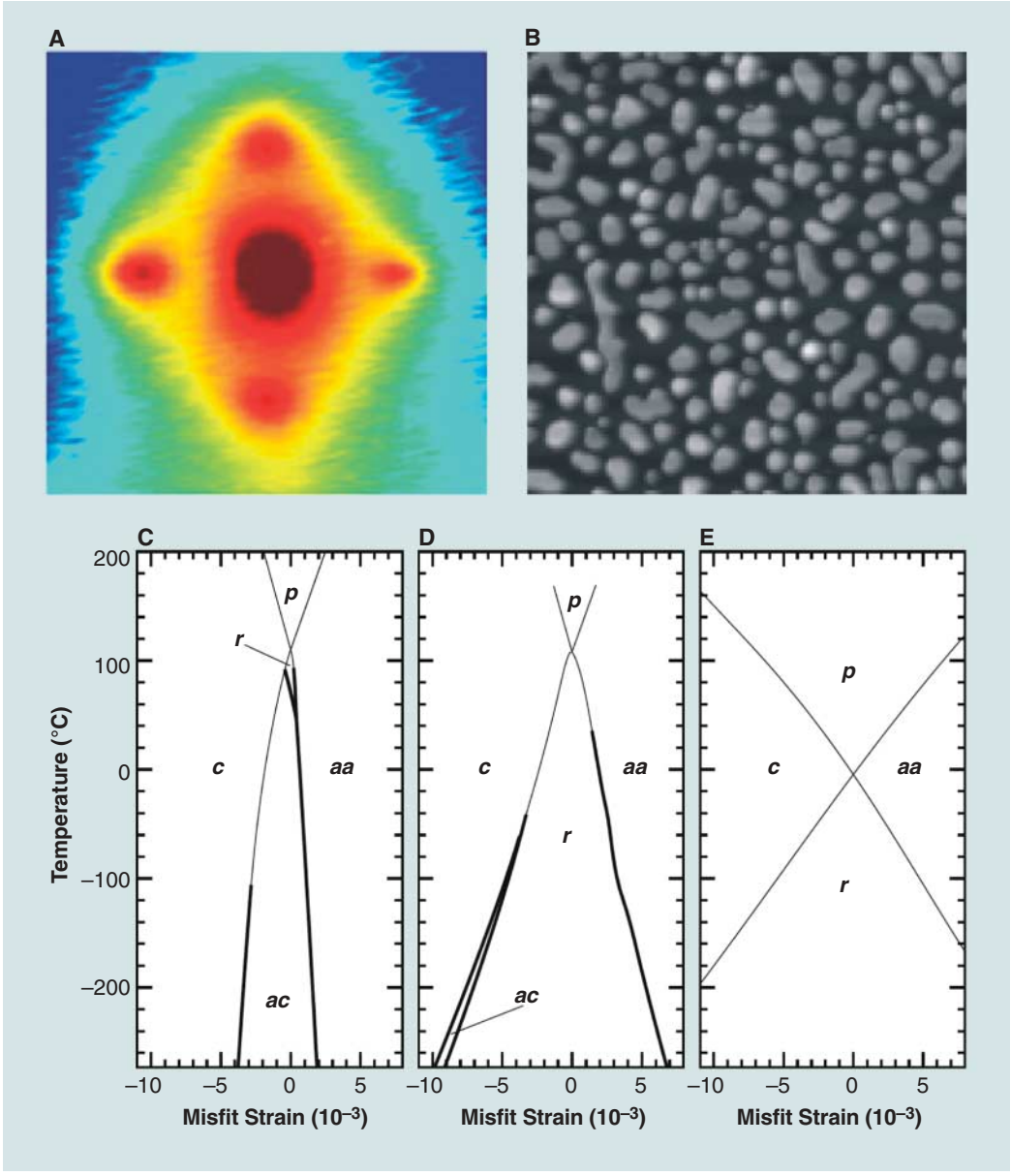

Fig. 3. Storage devices. (**A**) In-plane diffuse x-ray scattering profiles around the $PbTiO_3$ <303> Bragg peak at 549 K (*33*). The four satellite reflections are not Bragg peaks but instead are due to periodic stripe domains in orthogonal directions, and the geometry reveals that polarization *P* lies out of the plane of the film. (**B**) PZT self-assembly. AFM scan shows PZT on $SrTiO_3$ (*18*). Scale, 2.5 by 2.5 μm from left to right edge and from top to bottom edge of panel. (**C** to **E**) $BaTiO_3$ temperature-stress diagram with ab initio results (*29*) (E) and results from Pertsev and Tagantsev in 1998 (*28*) (C) and 1999 (*51*) (D).

Downloaded from www.sciencemag.org on March 1, 2007

Frenkel, and the films can be fully or partially depleted. Interfacial phenomena were recently reviewed (*33*). Early problems with fatigue, partially due to perovskite-pyrochlore conversion (*34*) in FeRAMs, have been overcome. Replacement of Pt by oxide electrodes to eliminate fatigue spawned a lot of good research, but Matsushita and Panasonic find the metallic Pt electrodes on SBT to be very satisfactory.

Ferroelectric superlattices. Artificially layered ferroelectric superlattices, such as $BaTiO_3/SrTiO_3$ can produce enhanced polarization P and dielectric constant ε. $PbTiO_3/SrTiO_3$ is particularly notable because it has a near-perfect lattice constant match (*35*). Surprisingly, the $SrTiO_3$ polarization in $BaTiO_3/SrTiO_3$ flops from along [001] to [110] in the relaxed superlattice (*36*, *37*), with strain energy overcoming electrostatics.

A related topic is periodically poled crystals of $LiNbO_3$ and other nonlinear optical materials (*38*). Here, the superlattice consists not of different chemical compositions such as $BaTiO_3/SrTiO_3$, but of $+P$ and $-P$ domains, providing efficient phase-matching for nonlinear optics. The quest at present is to produce submicrometer wavelengths and to understand domain widths and stability.

Ultrathin single crystals. The use of focused ion beams to cut nanoferroelectrics was pioneered by Ramesh's group in Maryland for ceramic films but recently extended to single crystals of $BaTiO_3$ (*39*) to characterize single-crystal capacitors of thickness down to about 65 nm. This has shown that effects of Curie temperature shift or dielectric peak broadening are extrinsic, contrary to the previous conventional wisdom.

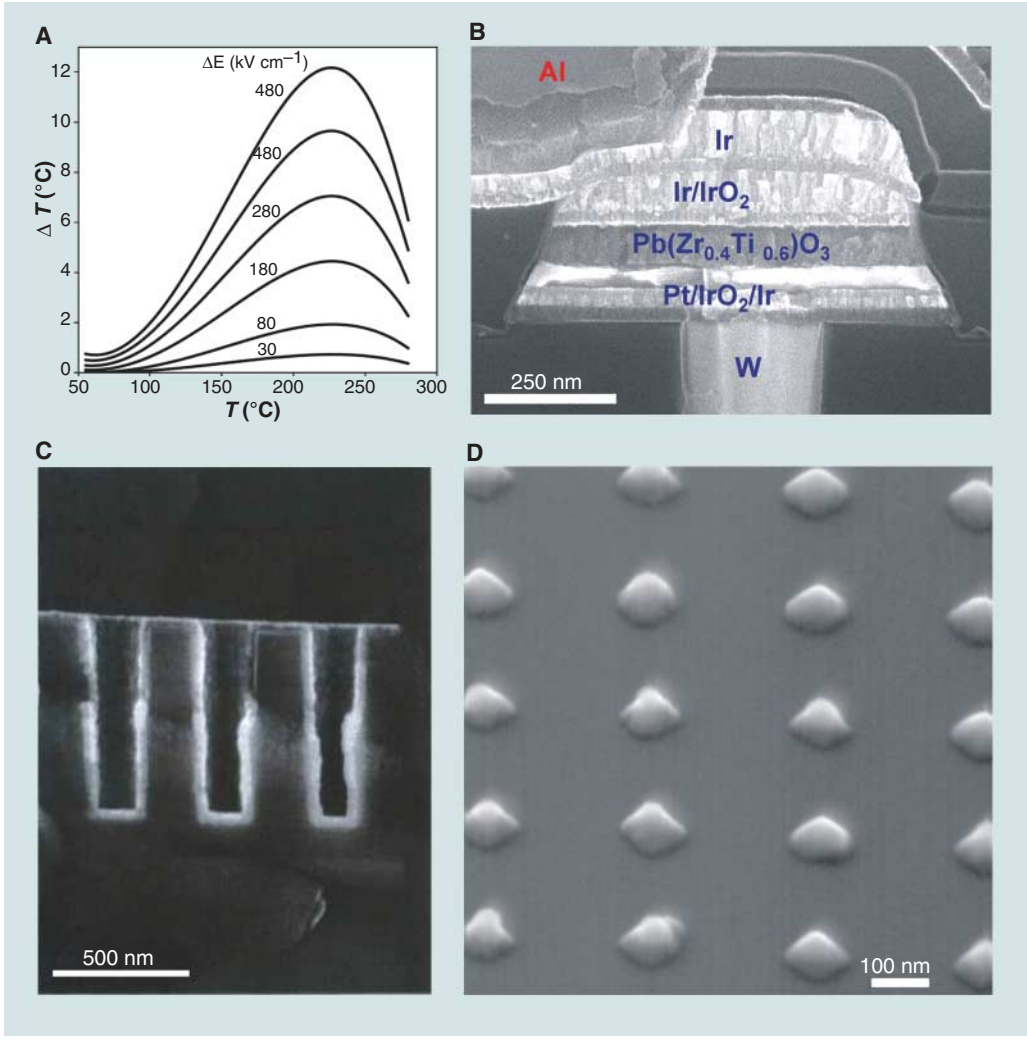

Fig. 4. Applications. (**A**) Electrocaloric effect in PZT (*39*). (**B**) SEM cross-section of 32 Mb Samsung PZT FeRAM (*52*). (**C**) SEM cross-section of ruthenium nanotrenches in Si (*53*). (**D**) e-beam lithography. Plan view shows PZT capacitor array (*54*).

Short-Term Applications

Electrocaloric cooling for mainframes and microelectric motors. The fact that ferroelectrics can be cooled by applying an electric field to them under certain conditions is termed the "electrocaloric effect." Using thermodynamics and the idea that entropy decreases under applied field E, one finds a temperature cooling of

$$\Delta T = T_1 - T_2 \approx [\beta T_1/(2c)][P_1^2(E) - P_2^2(0)] \quad (3)$$

where c is specific heat at constant polarization P, and β is the P^4 coefficient in the free energy $G(T,P) = \alpha(T - T_c)P^2 + \beta P^4$, so that ΔT is often measured from P rather than directly. Electrocaloric cooling was studied 1960s to 1970s, but the effect was small in bulk (a few millikelvin per volt). Recently however, Mischenko *et al.* measured $\Delta T = 12$ K at 25 V across 350 nm for cooling (Fig. 4A) in ferroelectric thin films (*40*), sufficient to design a prototype cooler for computer mainframes.

Electron emission from ferroelectrics. The fact that ferroelectrics emit copious electrons from their surfaces during switching has been known for many years. First discovered in Michigan by Rosenblum, this phenomenon was later investigated extensively at Centre Européen pour la Recherche Nucleaire (CERN) (*41*) and in France, Poland, Israel, and the United States. The prototype use as a synchronized, pulsed electron source for accelerators was investigated, including the extension to flat channel-plate structures. Currents of tens of amperes have been obtained with synchronized, monoenergetic pulse lengths of 100 ns to 1 μs. These are superior to thermionic cathodes in that they have higher current densities and lifetimes and also have instant turn-on (thermionic cathodes require a warm-up). The ferroelectric electron emitters can be operated in a poor vacuum and require no separate activation process. The commercial drawbacks are that the intense electric fields cause microcracking and device failure and that the effect is poorer in thin films than in bulk. Moreover, no unambiguous theoretical model has been accepted for the basic emission process. Microscopic mechanisms remain debatable. Although fields of $E = 10^7$ V/cm are required, this is only 50 V across 50 nm, readily obtainable in good films.

This is an unexploited device area for which commercial development of miniature high-power microwave devices could be made within a few years. Samsung explored in the 1990s the use of this phenomenon for nanolithography (*42*). Most recently (in 2005), this effect was used by Putterman's group for a kind of cold fusion (*43*), as a miniaturized source of x-rays and neutrons.

Base-metal-electrode capacitors. Barium-titanate–based ceramic capacitors are a commodity and account for the bulk of all condensers used in electronics (billions per year). These are

Downloaded from www.sciencemag.org on March 1, 2007

multilayer capacitors with Ag/Pd electrode stacks. Present efforts are to increase high-voltage performance to higher breakdown voltages and to further reduce costs by replacing silver-palladium with base metals, especially nickel. The electrode separation d varies from submicrometer to about 20 μm. Recently Milliken *et al*. have shown (*44*) that the breakdown field varies as the dc thermal model predicts (ignoring transient effects of applied field ramp rate): $E_B = c_1 d^{-1/2}$ for thicknesses above 1 μm, but no theory exists for the submicrometer-spaced devices, for which electrode surface roughness may be the limiting parameter. Progress can be expected in this high-volume commercial area in the next 5 years: Ni replacement, higher-breakdown devices, and a reliable theory for both Ni-$BaTiO_3$ interfaces and the nonmonotonic dependence of breakdown voltage on the electrode separation d. This has not been a trendy research area in universities, but the financial pay-off is potentially huge. Another major commercial area, not reviewed here, is piezoelectric actuators. Most piezoelectrics are ferroelectric, and new "relaxor" ferroelectrics such as lead magnesium niobate compounds achieve 2% strain, about 10 times that in conventional ferroelectrics. The most valuable application area is fuel injectors for automobile engines.

Phased-array radar. Thin-film ferroelectrics exhibit a large decrease in dielectric constant with application of modest voltages. This suggested that they could be used as the active phase-shift element in phased-array radar, a project studied carefully by researchers at Grumman and TRW in the United States and by Vendik's group in Leningrad. Unfortunately the dielectric loss tangent in these films remains too large for acceptable insertion losses in such devices, so nothing has been made commercially. A status report was published recently by Miranda *et al*. (*45*).

Future Prospects

Hybrid devices combining piezoelectric nanotubes with carbon nanowires will appear in 2007. Si_3N_4 dielectric capacitor tips on carbon nanotubes exist (*46*), and my group has put PZT tips on a registered array of carbon nanotubes. Commercial ferroelectric cells (up to 64 Mb) in FeRAMs are 0.4 μm (0.12 mm thick) in ceramic form (Samsung; Fig. 4B), 0.35 μm (Fujitsu), and 0.13 to 0.18 μm (Matsushita); thinner samples suffer from tunneling currents but may be useful for 3D DRAMs (Fig. 4C). Single crystals of ≈50 to 70 nm and films of ≈2 nm are under study, as are piezoelectric 3D nanotubes for microfluidics. Atomizers for insulin inhalers (e.g., Pfizer "Exubera," 2006) require small particles or droplets of uniform diameter, and the U.S. market for diabetes products (190 million cases worldwide) is $25 billion per year. Although microfluidics (including ink-jet printers) favor piezoelectric tubes of micrometer-sized diameters, microelectronics may exploit the smaller 5- to 10-nm-diameter rings and tubes shown here for DRAM trenching, with PZT/Pt-nanowire arrays recently giving nearly 1 Tb/in^2 nonvolatile memory arrays. Read-write speeds are already as fast as 280 ps for laboratory devices, but sense amplifier realities and bit-line capacitance limit commercial FeRAMs to about 5-ns access time. e-beam lithography (Fig. 4D) still leads self-assembly techniques for the registration required for commercial random access memories, but self-assembly with high registration will eventually win out. FeRAMs are way ahead of MRAMs, but multiferroic memories with electrical write and magnetic read operations may yet blossom.

References and Notes

1. A. von Hippel, "U.S. National Defense Research Committee Report 300" (NDRC, Boston, MA, 1944).
2. M. E. Lines, A. M. Glass, *Principles and Applications of Ferroelectrics and Related Materials* (Clarendon, Oxford, 1977).
3. Hence, the fashionable question "Why are there so few magnetic ferroelectrics" cannot have an answer limited to d^0-orbitals in transition-metal oxides (*47*).
4. Abrahams (*48*) indicates that several families of d-electron transition-metal fluorides are probably ferroelectric ferromagnets.
5. J. F. Scott, C. A. Araujo, *Science* **246**, 1400 (1989).
6. J. F. Scott, *Ferroelectric Memories* (Springer, Heidelberg, Germany, 2000).
7. M. Fiebig, *J. Phys. D* **38**, R123 (2005).
8. W. Eerenstein, N. D. Mathur, J. F. Scott, *Nature* **442**, 759 (2006).
9. C. A. Paz de Araujo, J. D. Cuchiaro, L. D. McMillan, M. C. Scott, J. F. Scott, *Nature* **374**, 627 (1995).
10. C. Kittel, *Phys. Rev.* **70**, 965 (1946).
11. G. Catalan, *Appl. Phys. Lett.* **88**, 102902 (2006).
12. V. A. Stephanovich, I. A. Lukyanchuk, M. G. Karkut, *Phys. Rev. Lett.* **94**, 047601 (2005).
13. H. Zheng *et al.*, *Science* **303**, 661 (2004).
14. P. Paruch, T. Giamarchi, J.-M. Triscone, *Phys. Rev. Lett.* **94**, 197601 (2005).
15. R. Pollard *et al.*, personal communication.
16. M. M. Saad *et al.*, *IEEE Trans. Ultrason. Ferroelectr. Freq. Control* **53**, 2208 (2006).
17. X. H. Zhu *et al.*, *Appl. Phys. Lett.* **89**, 129913 (2006).
18. M. Dawber, I. Szafraniak, M. Alexe, J. F. Scott, *J. Phys. Condens. Mat.* **15**, L667 (2003).
19. M. Tanaka, Y. Makino, *Ferroelectr. Lett.* **24**, 13 (1998).
20. F. D. Morrison, L. Ramsay, J. F. Scott, *J. Phys. Condens. Mat.* **15**, L527 (2003).
21. D. L. Fox, J. F. Scott, *J. Phys. C* **10**, L329 (1977).
22. C. Ederer, N. Spaldin, *Phys. Rev. B* **74**, 020401 (2006).
23. J. Hemberger *et al.*, *Nature* **434**, 364 (2005).
24. N. D. Mermin, *Rev. Mod. Phys.* **51**, 591 (1979).
25. R. J. Harrison, R. E. Dunin-Borkowski, A. Putnis, *Proc. Natl. Acad. Sci. U.S.A.* **99**, 16556 (2002).
26. M. Dawber, K. M. Rabe, J. F. Scott, *Rev. Mod. Phys.* **77**, 1083 (2005).
27. X. Wu, D. Vanderbilt, D. R. Hamann, *Phys. Rev. B* **72**, 035105 (2005).
28. N. A. Pertsev, A. G. Zembilgotov, A. K. Tagantsev, *Phys. Rev. Lett.* **80**, 1988 (1998).
29. O. Diéguez, K. M. Rabe, D. Vanderbilt, *Phys. Rev. B* **72**, 144101 (2005).
30. Y. L. Li *et al.*, *Phys. Rev. B* **73**, 184112 (2006).
31. M. Dawber, P. Chandra, P. B. Littlewood, J. F. Scott, *J. Phys. Condens. Mat.* **15**, L393 (2003).
32. J. Junquera, P. Ghosez, *Nature* **422**, 506 (2003).
33. O. Auciello, *J. Appl. Phys.* **100**, 051614 (2006).
34. X. Lou, M. Zhang, S. A. T. Redfern, J. F. Scott, *Phys. Rev. Lett.* **97,** 177601 (2006).
35. M. Dawber *et al.*, *Phys. Rev. Lett.* **95**, 177601 (2005).
36. A. Q. Jiang, J. F. Scott, H. Lu, Z. Chen, *J. Appl. Phys.* **93**, 1180 (2003).
37. K. Johnston, X. Huang, J. B. Neaton, K. M. Rabe, *Phys. Rev. B* **71**, 100103 (2005).
38. D. Walker *et al.*, *J. Phys. D Appl. Phys.* **38**, A55 (2005).
39. M. M. Saad *et al.*, *J. Phys. Condens. Mat.* **16**, L451 (2004).
40. A. S. Mischenko, Q. Zhang, J. F. Scott, R. W. Whatmore, N. D. Mathur, *Science* **311**, 1270 (2006).
41. H. W. Gundel, *Ferroelectrics* **184**, 89 (1996).
42. D. C. Kim, W. Jo, H. M. Lee, K. Y. Kim, *Integ. Ferroelectr.* **18**, 137 (1997).
43. B. Naranjo, J. K. Gimzewski, S. Putterman, *Nature* **434**, 1115 (2005).
44. A. D. Milliken, A. J. Bell, J. F. Scott, *Appl. Phys. Lett.*, in press.
45. A. L. Morales-Cruz *et al.*, *Integ. Ferroelectr.* **77**, 51 (2005).
46. T. Ami *et al.*, *Integ. Ferroelectr.* **14**, 95 (1997).
47. N. Hill, *J. Chem. Phys. B* **104**, 6694 (2000).
48. S. C. Abrahams, *Acta Crystallogr.* **B55**, 494 (1999).
49. G. Catalan, J. F. Scott, A. Schilling, J. M. Gregg, *J. Phys. Condens. Matter* **19**, 022201 (2007).
50. M. Dawber, N. Stucki, C. Lichtensteiger, J.-M. Triscone, personal communication.
51. N. A. Pertsev, A. G. Zembilgotov, A. K. Tagantsev, *Ferroelectrics* **223**, 79 (1999).
52. J. F. Scott, *J. Phys. Condens. Mat.* **18**, R361 (2006).
53. K. Kawano, H. Kosuge, N. Oshima, H. Funakubo, *Electrochem. Sol. St. Lett.* **9**, C175 (2006).
54. M. Alexe, C. Harnagea, D. Hesse, U. Gösele, *Appl. Phys. Lett.* **79**, 242 (2001).

25 July 2006; accepted 1 November 2006
10.1126/science.1129564

Downloaded from www.sciencemag.org on March 1, 2007